JOURNAL OF MATERIALS SCIENCE 11 (1976) 2198–2210

Micromechanics of solvent crazes in polystyrene

HEIDER G. KRENZ, DIETER G. AST, EDWARD J. KRAMER
Department of Materials Science and Engineering and the Materials Science Center, Cornell University, Ithaca, New York, USA

Double exposure holographic interferometry (DEHI) is used to determine the strain energy release rate, craze opening displacement profile, and craze stress profile of *n*-heptane and methanol crazes growing from cracks in polystyrene. *n*-heptane crazes have strain energy release rates (SERRs) close to those of cracks and their stress profile is almost crack-like in that the tensile stress across the craze falls almost to zero. On the other hand, the SERRs of methanol crazes are only 30 to 55% the SERR of a crack depending on stress intensity factor K_I of the precrack from which they are grown. The stress profile of the methanol craze shows it to be strongly load-bearing away from the craze tip, apparently as a result of the strain hardening of the craze fibrils. The stress concentration in front of the methanol craze tip is only 40% of that in front of the *n*-heptane craze tip. The opening displacements of the methanol craze are almost as large as those of a crack very near its tip but are much less than those of a crack at large distances behind the tip. The Dugdale model of a strip yielding zone provides a poor representation of the craze opening displacements of the growing methanol craze. Dry (static) methanol crazes have larger opening displacements in response to an incremental tensile strain at moderate prestrains than at either low or high prestrains, suggesting that the craze fibrils undergo a yielding/strain-hardening process as the strain is increased similar to that observed in polycarbonate crazes by Kopp and Kambour. Dry *n*-heptane crazes do not show this response but rather open linearly with increasing prestrain. The opening displacement for long (dry) *n*-heptane crazes is almost crack-like whereas the largest opening of a dry methanol craze is only ~ 20% of that of a crack. Dry methanol crazes break at a K_{IC} that is ~ 40% of the K_{IC} of precracked but uncrazed specimens. The strongest (shortest) dry *n*-heptane crazes fail at only ~ 7% of K_{IC} of uncrazed specimens and the K_{IC} of the dry *n*-heptane crazes decreases markedly with increasing craze length.

1. Introduction

The mechanical behaviour of crazes in glassy polymers is important to all aspects of the fracture processes in these materials. It is now widely accepted that the relatively high fracture toughness of these materials is due to the plastic work done in generating a craze (or crazes) in front of the advancing crack tip. This plastic work in turn depends on the mechanical properties of the crazes, specifically the stress–craze opening displacement relationship. Information on the craze opening displacement profile is necessary to test models, such as the Dugdale model, which can predict the fracture toughness.

On the other hand, it is also well established that cracks usually initiate within mature crazes. For knowledge and control of the processes leading to crack initiation, information is necessary on the thinning and plastic rupture of craze fibrils

and the corresponding loss of load-bearing capacity of the mature craze.

Finally, the mechanical properties of the craze must affect the kinetics of its growth. It has been proposed, for example, that by analogy to crack growth, there exists a critical strain energy release rate G for craze growth [1]. Unlike the G for a crack which can be computed from geometry and loading information, the G for a craze must be measured experimentally.

Double exposure holographic interferometry is a technique which can be used to determine all the mechanical properties of crazes outlined above and one of the purposes of this paper is to demonstrate this fact. However, it is often tacitly assumed that the properties of crazes in a given polymer are similar regardless of the conditions (solvent, stress, temperature) under which they are grown. If this were the case the techniques outlined here would be of rather limited practical usefulness. We shall demonstrate, however, that crazes produced by different crazing agents in the same polymer have completely different mechanical properties. The holographic techniques described here appear to be the only practical means of rapidly detecting these differences.

2. Specimen preparation

Commerical polystyrene sheet ($\bar{M}_w = 314 \times 10^3$, $\bar{M}_n = 97.8 \times 10^3$) is cut into tensile strip specimens (0.75 mm x 160 mm x 16 mm). A notch is cut in one edge at the middle of the specimen. Then the specimen is annealed at 85° C for 1 h between heavy brass plates and cooled in the furnace to room temperature at a cooling rate of approximately $20^\circ\,C\,h^{-1}$. This treatment removes residual stresses in the specimen due to moulding and heals out crazes at the notch tip introduced due to the cutting procedure. The specimen is inserted into a tensile strain frame which consists of two translation stages mounted on a back plate (Fig. 1). The position of the stages is measured by two dial gauges independent of the driving mechanism. A small tensile strain is applied symmetrically by translating both stages the same amount. A single craze is grown from the notch by supplying *n*-heptane to the notch via a wick. The craze is dried for 1 h and then fractured by applying a small additional strain producing a single sharp crack. The specimen is removed from the strain frame and the heat-treatment at 85° C is repeated to heal out small crazes at the crack tip caused by the cracking of the *n*-heptane craze. The specimen is painted white on one side over its gauge length to enhance reflectivity during the holographic experiment. The specimen is again inserted into the strain frame on the optical table.

3. Double exposure holographic interferometry

Double exposure holographic interferometry (DEHI) is a method to determine small incremental displacements. The elements of the optical system are shown in Fig. 2. The beam of a Ar-ion laser is split into three beams which are expanded and filtered by spatial filters and then are collimated

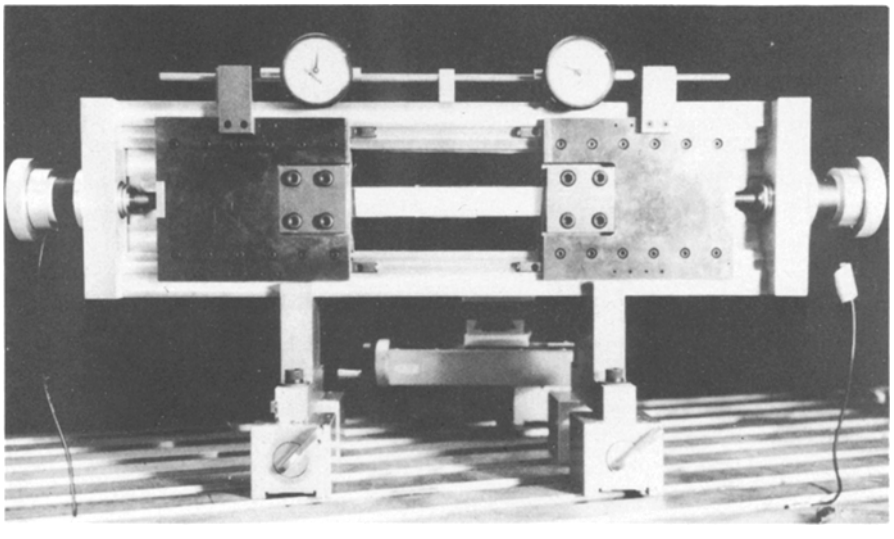

Figure 1 Photograph of the strain frame.

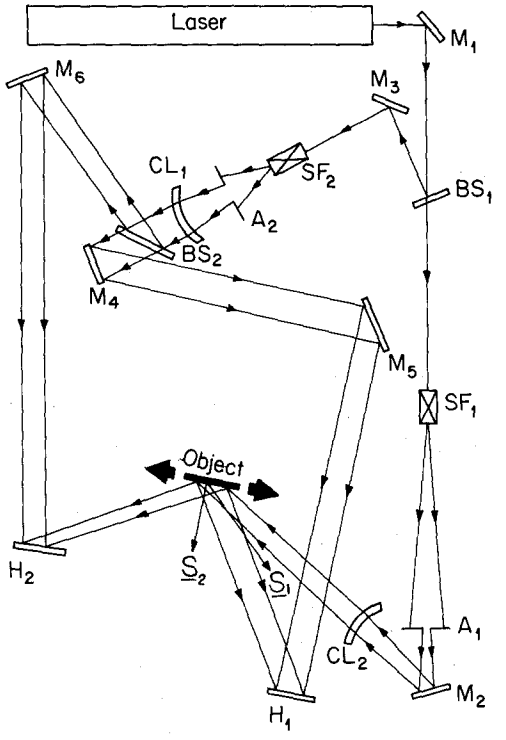

Figure 2 Holographic system: M = mirror, BS = beam splitter, SF = spatial filter, A = aperture, CL = collimating lens, s = sensitivity vector, H = holographic plate.

by convex lenses which have their focal points in the pinholes of the spatial filters. One beam serves as an illuminating beam which hits the specimen at an oblique angle. The two other beams serve as reference beams and form, with the reflected beams from the specimen, the holograms H_1 and H_2.

To take the double exposure hologram (DEH) a photographic plate is exposed simultaneously to the reference beam and to the reflection from the specimen. Then the state of strain of the specimen is changed and the exposure is repeated. The interference patterns resulting from these two exposures are recorded on the photographic plate. After being developed, the plate is rotated by 180° and placed again in the reference beam, whereupon a real image of the specimen is formed (reconstructed) in space. Superimposed on the image are fringes due to the displacement of surface points between exposures. Each fringe corresponds to a constant displacement of surface points in the direction of the sensitivity vector s which is the vector bisecting the angle 2θ between the illuminating and the reflected (or object) beam to the hologram. The increment of the displacement between neighbouring fringes in the direction of its sensitivity vector is given by

$$\delta u_s = \frac{\lambda}{2 \cos \theta}. \tag{1}$$

The wavelength of our Ar-ion laser is $\lambda = 4880$ Å. The in-plane component of the incremental displacement is then:

$$\delta u = \frac{\lambda}{2 \cos \theta \cos \alpha} = \Lambda, \tag{2}$$

where α is the angle between the tensile axis of the specimen and the sensitivity vector s. The increment in normal strain between exposures in the y-direction is given by:

$$\delta \epsilon_{yy} = \Lambda / \Delta y \tag{3}$$

where Δy is the fringe spacing along the tensile axis. From the hologram one measures an apparent fringe spacing Δy_a, because it is viewed under an angle $\beta = \alpha + \theta$. The incremental strain therefore becomes:

$$\delta \epsilon_{yy} = \frac{\Lambda \sin \beta}{\Delta y_a}. \tag{4}$$

More detail of this calculation is given in [2] but it should be noted that the Equations 1 and 2 in [2] are misprinted. H_1 measures displacements with both in-plane and out-of-plane components, whereas H_2 is arranged such that it only measures out-of-plane displacements. Because in our type of experiment out-of-plane displacements are only due to undesired motions of the specimen, we use H_2 as a control hologram. When H_2 is fringe-free one can calculate, using Equation 2, the in-plane displacement component of a given point on the surface in the direction of the tensile axis from the reconstruction of H_1. Only holograms from experiments where H_2 was fringe-free were analysed.

Besides the general problems in DEHI of preventing instabilities of the laser, vibrations of the optical bench and shifting of the optical components in the time between exposures, special sources of possible error arise in our experiments. Bending of the backplate of the strain frame, misalignment of the translation stages or rotation of the grips on the translation stages can cause erroneous fringes. The strain frame was reconstructed several times until the DEH of grips, backplate and translation stages were fringe-free when increments of force larger than the largest experimental increments were applied to a test specimen without

a craze. During the actual experiments parts of the straining system that are in the field of view are constantly monitored for undesired displacements. Erroneous in-plane fringes also may be introduced by creep of the specimen material out of the grips between exposures. To eliminate this source of error uncrazed test specimens are strained a certain amount and the first exposure is taken. The second exposure is made after a time which is longer than the time of our longest experiment. By repeating this experiment at higher and higher load levels, a critical load level is found at which creep from the grips begins to be discernable. This load level is two times higher than the highest load level at which the present experiments are conducted.

A warped specimen can undergo large out-of-plane displacements with small changes in tensile load; these are readily detected by fringes in the out-of-plane hologram H_2. Warping of the specimen has been eliminated by annealing and slowly cooling it between heavy brass plates.

Measurements on growing crazes are most easily performed when the craze growth is caused by introduction of a liquid crazing agent to the crack tip via a wick. In this way crazes can be grown at low loads which minimize creep from the grips but the liquid causes two other problems. The crazing agent can interact with the paint, causing blistering. Therefore, a narrow path along the direction of the expected craze propagation is masked during the painting process by covering it with tape. Application and removal of the crazing agent also causes local thermal contraction and expansion of the specimen due to the local cooling caused by the evaporation of the crazing agent. These thermal strains can produce an extraneous fringe pattern. However, we have determined that the fringe pattern of a DEH taken before and after drying is exactly the same regardless of whether a crazed or a precracked specimen of the same geometry (craze length = crack length) is used. The fringe pattern produced on drying a craze under stress where no craze growth occurs is, therefore, entirely of thermal origin. No detectable craze or crack opening (or closing) displacements are observed that can be attributed to retraction (or healing) of the craze matter. The correct craze opening displacements due to craze growth can be determined by taking one exposure of the DEH before applying the crazing liquid and one exposure after the craze has been allowed to come to thermal equilibrium. Our experiments establish that thermal equilibrium is achieved for dried methanol and *n*-heptane crazes in ~ 3 min.

4. Experimental procedure and results

4.1. Holography of growing crazes

4.1.1. Definitions and procedures

According to linear elastic fracture mechanics, the strain energy release rate (SERR) of a crack is defined as:

$$G \equiv -\frac{\mathrm{d}W}{\mathrm{d}A} \tag{5}$$

where $\mathrm{d}W$ is the change of strain energy of the specimen due to the change in crack area $\mathrm{d}A$ [3]. Correspondingly, the SERR of a propagating craze can be evaluated by applying the standard methods of fracture mechanics. The SERR is given by

$$G = \frac{P^2}{2}\frac{\mathrm{d}J}{\mathrm{d}A}. \tag{6}$$

P is the tensile force, J is the compliance of the (crazed) cracked specimen and A is, in our case, the area of the craze instead of the crack. Substituting the relation $JP = \Delta$ where Δ is the displacement of the grips yields:

$$G = -\frac{\Delta}{2}\frac{\mathrm{d}P}{\mathrm{d}A}\bigg|_{\Delta=\mathrm{const}}. \tag{7}$$

The change in tensile force can be calculated from Hooke's law if the average released tensile strain $\langle \delta\epsilon_{yy} \rangle$ far from the craze is known.

The precracked specimen is inserted into the strain frame and a tensile load is applied. The load corresponds to a stress intensity factor K_I which is well below the critical stress intensity factor $K_{IC} = 1.2\,\mathrm{MN\,m^{-3/2}}$ for dry crazing in PS. The stress intensity factor is calculated from applied load and the precrack length using Brown and Srawley's formula [4]. The grip position is then held constant for the rest of the experiment and the first exposure of the DEH is made. A wick is brought into contact with the precrack and a crazing agent (methanol or *n*-heptane) is applied. In the case of methanol a short (~ 1 mm) craze grows almost instantaneously out of the crack tip. Longer crazes are usually accompanied by side crazes to form a narrow bundle. Only experiments in which single crazes propagated were used for evaluation. A single craze of arbitrary length usually can be grown at very low loads with *n*-heptane as the crazing agent. The craze growth is observed and measured with a telemicroscope

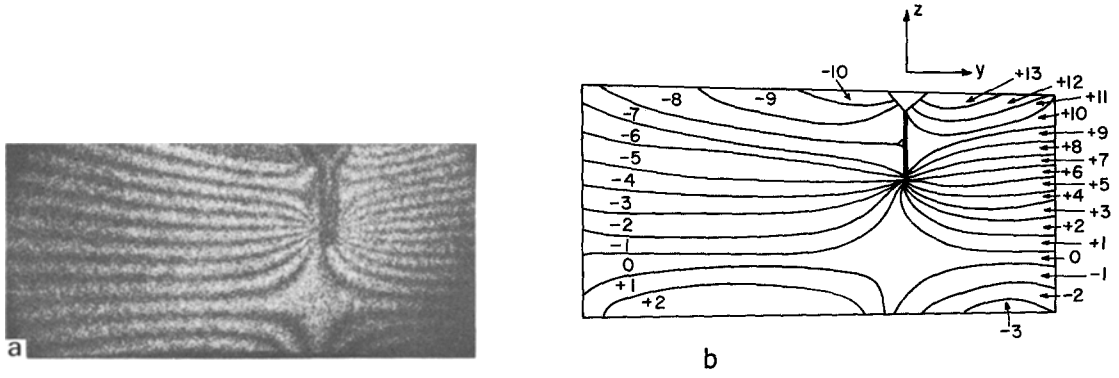

Figure 3(a) Double-exposure hologram of specimen with propagating craze. (b) Schematic of (a) with fringe order labelled.

while the holographic plates are shielded in light traps. After the craze has reached the desired length the crazing agent is removed, the specimen is dried until thermal equilibrium has been reached, and the second exposure of the DEH is made.

Reconstruction of the hologram (Fig. 3a) shows an image of the specimen and superimposed fringes which are caused by surface displacements due to the propagating craze. In Fig. 3b a schematic pattern is shown with the fringe order n labelled. The in-plane displacement u_y along the tensile axis in the $+y$ direction is given by

$$u_y = n\Lambda \tag{8}$$

where Λ, the displacement increment between fringes, is in this case 0.33 μm.

4.1.2. Expected results

As a further qualitative check on the validity of the fringe pattern for a propagating craze, the fringe pattern expected for a propagating crack has been computed using a finite element analysis program [5]. This pattern for a propagating crack is expected to be qualitatively similar to that for a propagating craze well away from the craze/crack. The specimen surface is covered with a rectangular grid and the differential displacements of the nodal points of the grid are calculated when a crack increases in length under constant grip displacement. One half of the specimen is shown in Fig. 4. The grid size is indicated in the lower left corner. Because of the coarse grid, the program is not expected to yield meaningful results in the immediate surroundings of the crack. Some lines of constant displacement are indicated with an arbitrary, but constant, displacement increment between them, but are not extended into the crack. Comparison of the computer finite element results with the actual pattern shows good qualitative agreement.

Note that the zero fringe indicating zero displacement forms a cross in front of the crack/craze tip, the two arms of which extend to and broaden at the grip showing that there is no grip

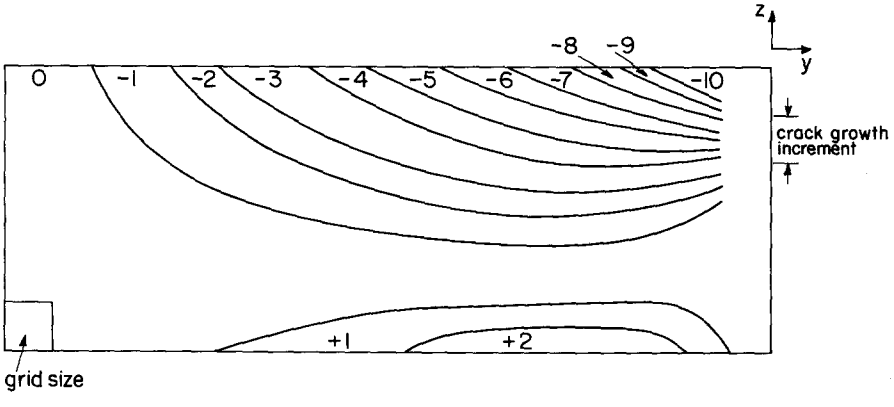

Figure 4 Left half of specimen with propagating crack. Fringes are calculated using finite element analysis. The displacement increment between fringes is arbitrary but constant.

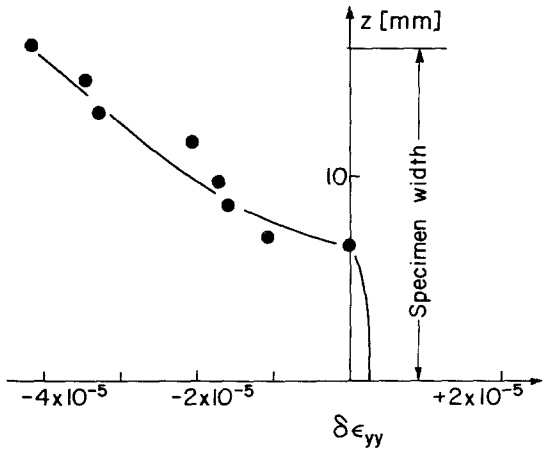

Figure 5 Profile or released strain $\delta\epsilon_{yy}$ due to craze propagation measured along a line y = const.

movement. The position of the zero fringe provides a good check of the symmetry of our loading system. The change from positive to negative displacement fringes along the z-axis shows that there is a considerable bending moment due to the craze/crack opening under fixed grip constraints. Another important feature that can be seen very well both in the computer results and in the actual pattern is that low order positive fringes exhibit a distinct minimum ($dz/dy = 0$) whereas higher order positive fringes enter the crack/craze with a constantly decreasing slope.

4.1.3. Evaluation of the strain energy release rate G

In order to find the average released strain $\langle\delta\epsilon_{yy}\rangle$ the spacing between neighbouring fringes is measured along a line parallel to the crack and craze. Dividing Λ, the in-plane surface displacement between fringes by the fringe spacing yields the change of strain at a particular point of the line (Equation 4). A plot of $\delta\epsilon_{yy}$ at points along the line gives the released strain profile at y = constant. A typical plot corresponding to the sample of Fig. 3 is given in Fig. 5. From such plots one can determine the average released strain $\langle\delta\epsilon_{yy}\rangle$ across the cross section of the sample. Although the profile of $\delta\epsilon_{yy}$ changes with different y-coordinates of the measuring line, the average released strain $\langle\delta\epsilon_{yy}\rangle$ is always the same. For convenience we always measure along a line at $y = w$, where w is the sample width. The graphical integration of the area in Fig. 5 can be approximated by a more convenient numerical integration if the number of fringes is large. The averaged released strain is given by:

$$\langle\delta\epsilon_{yy}\rangle = \Lambda \sin\beta\left(\frac{1}{w}\int_0^w \frac{1}{\Delta y_a}\,dz\right). \qquad (9)$$

The term in parenthesis can be approximated by the sum $(1/w)\,\Sigma(\Delta z/\Delta y_a)$, where Δz is the z-distance between neighbouring fringes. Using the angle γ between the tensile direction and the tangent of the fringe at the intersection of the fringe with the line y = constant, Equation 4 becomes:

$$\langle\delta\epsilon_{yy}\rangle = \Lambda\,(\sin\beta)\,\frac{\Sigma\tan\gamma}{w}. \qquad (10)$$

The average released strain calculated from this method is within 10% of the results from the graphical integration. Having found $\langle\delta\epsilon_{yy}\rangle$ the SERR is computed following Equation 7. Fig. 6a shows the results of these measurements. The SERR of propagating methanol and n-heptane crazes is plotted versus the square of the stress intensity factor K_I^2, where K_I again has been calculated from the applied load and the precrack length. In Fig. 6a the full circles and the full squares refer to the methanol crazes and to the n-heptane crazes, respectively. For comparison, the SERR for propagation of the precrack an infinitesimal distance is given by the straight line. This SERR has been calculated using

$$G = K_I^2/E \qquad (11)$$

for the case of plane stress, where E is Young's modulus of PS ($2.75 \times 10^3\,\mathrm{MN\,m^{-2}}$). It would appear that the SERRs of n-heptane crazes are higher than those of cracks, which is clearly impossible.

However, G for the craze as computed is not a true differential quantity but rather $\Delta W/\Delta A$ where the incremental growth area ΔA is large especially for n-heptane crazes. The G for craze growth should be compared with the average SERR, $\langle G\rangle$ for a crack propagating over the finite craze length increment Δa. A straightforward calculation based on Srawley and Brown's formula yields

$$\langle G\rangle = E^{-1}\left\{K_I^2 + \sigma^2\left[\frac{c_0}{2}\Delta a + \frac{2c_1c_0}{w}\Delta a a_0 + \frac{3}{2w^2}\left(c_1^2 + 2c_0c_2\right)\Delta a a_0^2 + \frac{2c_1c_0}{3w}\Delta a^2 + \left(\frac{c_1^2 + 2c_0c_2}{w^2}\right)\left(\Delta a^2 a_0 + \frac{\Delta a^3}{4}\right)\right]\right\} \qquad (11a)$$

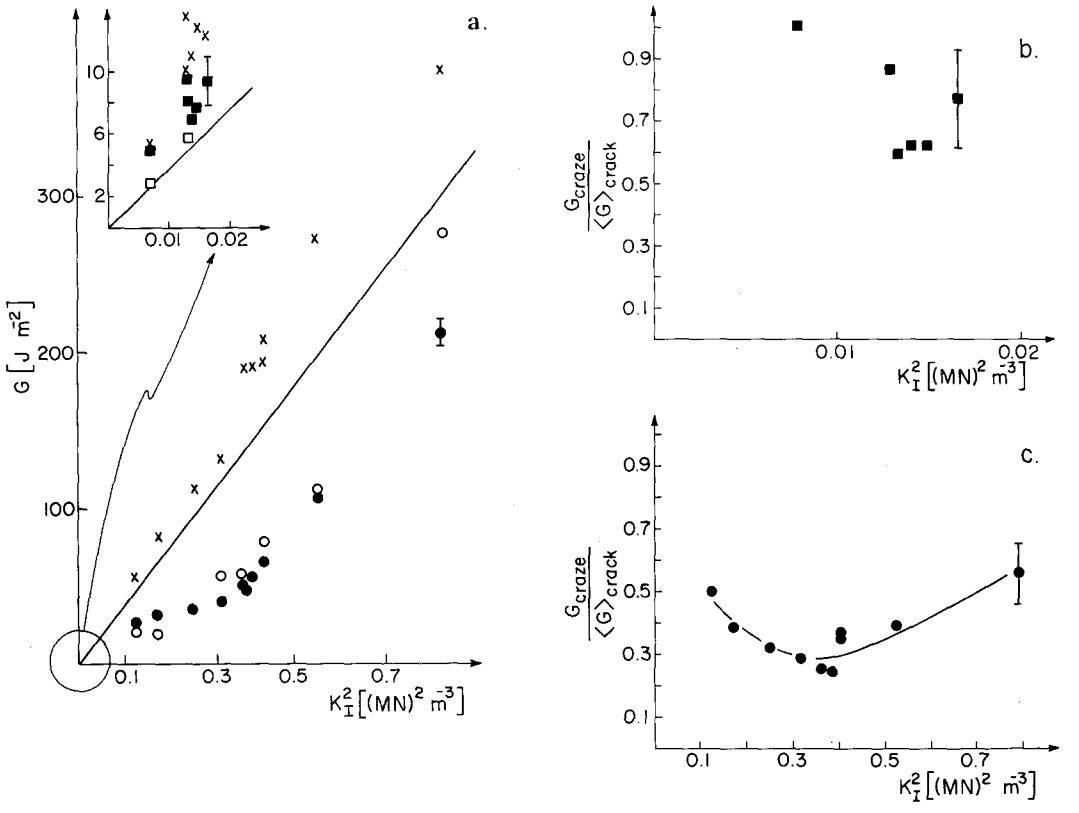

Figure 6(a) Strain energy release rate G versus square of the stress intensity factor K_I^2. ■ and ● are experimental data for propagating *n*-heptane crazes and methanol crazes, respectively, computed from $\langle \delta \epsilon_{yy} \rangle$ and Equation 7. □ and ○ are data for propagating *n*-heptane crazes and methanol crazes, respectively, computed from the opening displacement of the precrack base; the straight line and × represent data for a crack calculated from Equations 11 and 11a, respectively. Typical error bars are indicated. (b) Normalized strain energy release rate of *n*-heptane crazes versus K_I^2. (c) Normalized strain energy release rate of methanol crazes versus K_I^2. Note different scales of abscissa in (b) and (c).

where σ is the stress applied at the grips, K_I is the stress intensity factor, and a_0 is the length of the precrack. The constants from [4] are $c_0 = 1.99$, $c_1 = 0.41$ and $c_2 = 18.70$. Average SERR values for cracks calculated with Equation 11a are shown with crosses in Fig. 6a. In the case of *n*-heptane crazes these values are 100% higher than the differential SERR (Equation 11).

Our measured craze SERRs can be checked by an alternate method. A normalized crack opening is defined as the crack opening displacement divided by the sample thickness and by the applied tensile strain causing this opening. Following Brown and Srawley [4], a plot of normalized crack opening at the crack base versus the ratio of crack length to specimen width (a/w) is established for our loading system by taking double exposure holograms of specimens with different (a/w) ratios, where a small incremental strain is applied between exposures. The opening displacement at the base can be calculated with Equation 8 after having counted the number of fringes that enter the crack. Knowing the ratio of the starter crack length to specimen width yields an initial value of the normalized opening. The DEH due to the craze propagation under fixed grip position gives an additional incremental normalized opening if the fringes that enter the crack are counted and Equation 8 is applied again. From this increment we can calculate how much a crack would have to propagate in order to cause the measured opening at the base of the real craze and crack. In all cases this ficticious crack advance is smaller than the actual craze advance. The SERR of the craze is the SERR of the crack times the ratio of the ficticious crack growth increment to the actual craze growth increment. The SERR of the craze computed by this method is shown in Fig. 6a for some of the methanol and *n*-heptane crazes by open circles and open squares, respectively. These

results are in basic agreement with our directly measured SERR values.

The fractional craze SERR, defined as $G_{craze}/\langle G\rangle_{crack}$, is plotted versus K_I^2 in Fig. 6b and c for *n*-heptane and methanol crazes, respectively. The SERR of the *n*-heptane crazes is almost as large as that of a crack even at very low K_Is. The SERR cannot be established for higher K_Is for *n*-heptane, because multiple crazing or fracture by crack propagation is produced. On the other hand, the SERR for methanol crazes is much lower than that of a crack and is not a constant fraction of $\langle G\rangle_{crack}$.

4.1.4. Craze opening displacement of propagating crazes

The craze opening displacement profile of the growing craze can also be determined directly with DEHI. Starting in Fig. 3 from the zero fringe at the tip of the craze one can determine the fringe order at every point along both sides of the craze. Because each fringe is a line of known constant displacement in the tensile direction (Equation 8), this procedure yields the absolute craze opening displacement. Although fringes also enter the crack due to the crack opening with craze propagation, we count only fringes from the tip of the craze to its base; thus only the opening displacement of the craze is plotted versus the normalized craze length. Typically the craze opening displacement increases rapidly at the tip and more slowly near the base. The craze opening can be compared with the crack opening displacement calculated from linear elastic fracture mechanics (see for example, [6]). That crack opening displacement for a crack length equal to the precrack length plus the craze length is shown as curve a in Fig. 7. In the case of the crack the normalized distance $z/a = 1$ corresponds to the opening of the crack at a distance equal to the craze length behind the crack tip. It shows that the craze opening is approximately crack-like at its tip but is less than one quarter the crack opening at its base. It should be noted that the absolute craze opening displacement does not give any information about the craze strain, because the initial width of polymer that finally transforms into craze matter is not known.

4.1.5. Dugdale model

Attempts have been made to compare crazing ahead of the crack tip to the Dugdale model of strip zone yielding. Brown and Ward [7] have estimated the craze opening displacement u from the optical thickness of crazes grown in air in PMMA and find good agreement with the predictions of the Dugdale model. The craze opening u can be calculated using:

$$u = \frac{8\sigma_f a}{\pi E}\left\{\left(\frac{z}{a}\right)^{1/2} - \left(\frac{1-z/a}{2}\right)\ln\left[\frac{1+(z/a)^{1/2}}{1-(z/a)^{1/2}}\right]\right\} \quad (12)$$

where z/a is the normalized craze length, a is the craze length, and E is Young's modulus ($2.75 \times 10^3\,MN\,m^{-2}$). The stress σ_f is the flow stress of the material in the plastic zone. The length of the plastic zone (craze) is predicted to be: $a = \pi K_I^2/8\sigma_f^2$. Using the length of the craze and the applied stress intensity factor we can substitute for σ_f in the Equation 12. A plot of the calculated craze opening displacement according to the Dugdale model versus normalized craze length is given in Fig. 7, curve c, where we have used the craze length and stress intensity factor of the specimen shown in Fig. 3. The comparison of the calculated opening with the real opening (Fig. 7, curve b) clearly shows that the predicted openings from the Dugdale model are much smaller than the measured

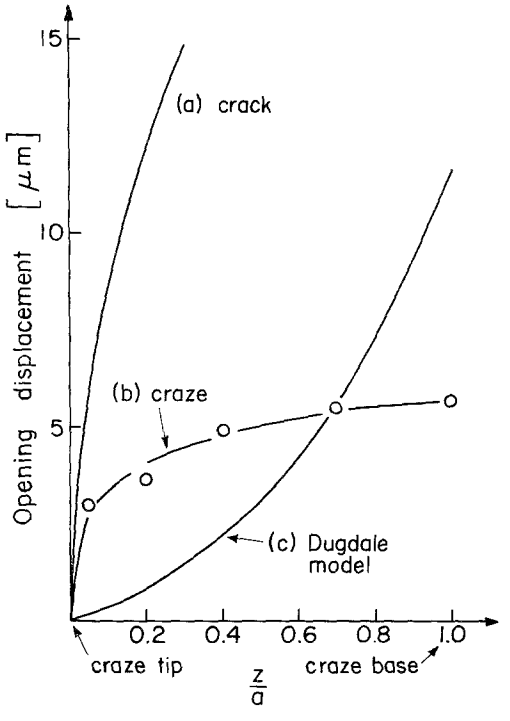

Figure 7 Opening displacement versus normalized distance z/a. (a) represents the calculated opening of the crack tip of a crack of length = precrack + craze, (b) is the measured opening of the craze in Fig. 3, (c) is the craze opening calculated from Equation 12.

openings near the craze tip and larger near the craze base. The reason for the large discrepancy near the craze tip lies in the assumption of the Dugdale model that the strip of material ahead of the crack tip is a perfectly elastic/plastic solid with a flow stress σ_f which does not vary with position ahead of the crack. In solvent crazing this assumption is violated because the flow stress (or crazing stress) of the material is lowered by plasticization with the crazing liquid only in the vicinity of the craze tip. Although this zone of plasticization (and lower σ_f) extends further from the crack tip as the craze grows, the kinetics of this extension are dependent on the transport of the crazing agent within the craze to its tip [8] and the diffusion of the crazing agent into the polymer at the tip of the craze. Since we only apply the crazing agent for a limited time, the craze growth is stopped before the craze could grow to its equilibrium length. This case of the equilibrium craze length is the only case where the Dugdale model can be expected to apply. The discrepancy near the craze base between the measured opening and the larger value predicted by the Dugdale model has a different origin and will persist even for a craze of equilibrium length. It is due to the strong strain-hardening of the craze fibrils near the base of the craze, the existence of which will be shown in the next section where the stress profile along the craze length is determined.

4.1.6. Stress profile of growing crazes

From the DEH given in Fig. 3 it is possible to approximately determine the change in tensile stress $\delta\sigma_{yy}$ due to the propagating craze. Using Hooke's law the change in stress in the longitudinal direction for the case of plane stress is given by:

$$\delta\sigma_{yy} = E\delta\epsilon_{yy}\left(\frac{1+\nu\dfrac{\delta\epsilon_{zz}}{\delta\epsilon_{yy}}}{1-\nu^2}\right). \qquad (13)$$

Previous experiments [2] have shown that $\delta\epsilon_{zz}/\delta\epsilon_{yy} = -\nu$ is reasonably satisfied such that the change in stress can be approximated to be:

$$\delta\sigma_{yy} = E\delta\epsilon_{yy}. \qquad (14)$$

The change in strain along a line parallel to the craze of Fig. 3 ($y = 0.32$ mm) has been measured. One can see from Fig. 3 that close to the base of the craze, fringes enter that have a constantly decreasing positive slope until fringes $n = +5$ and $n = -5$ which enter the craze at zero slope. Close to the craze tip the fringes enter with an increasingly negative slope. In the first region measurements of the fringe spacing along a line y = constant will go from fringes of higher order to fringes of lower order, indicating decreasing strain in this regime. In the second regime the fringe spacing is measured between increasing fringe numbers. The change in strain here is therefore positive. The change in strain is subtracted from the strain profile determined from a DEH of a crack of the length of our precrack under the applied load of our experiment. Fig. 8 shows the initial strain profile of the crack and the changed strain profile due to the methanol craze propagation in the strain field of the crack. The corresponding stresses as calculated with Equation 14 are also given. As expected the stress is only slightly relieved over most of the craze length, but more strongly relieved just behind the craze tip, where the craze opening is more crack-like (see Fig. 7, curve a). The decrease of stress in this region may be even higher at the craze plane but the fringe spacing closer to the craze cannot be resolved. Ahead of the craze the stress increases and there is a stress concentration of about 1.6 compared with the stress ahead of the crack before craze growth. The stress concentration in the immediate

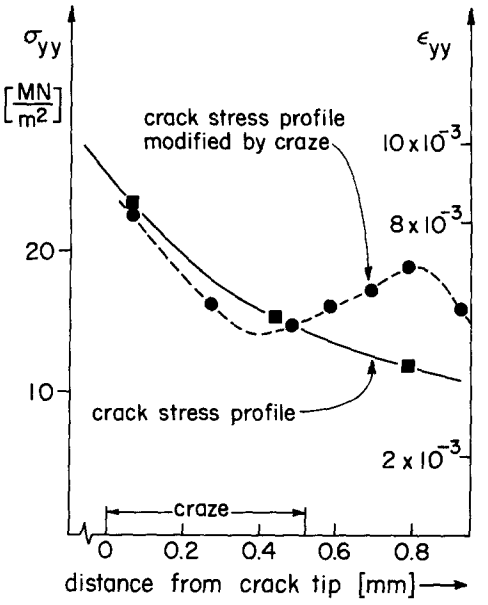

Figure 8 Stress and strain profile versus distance from crack tip along a line parallel to the propagating methanol craze in Fig. 3.

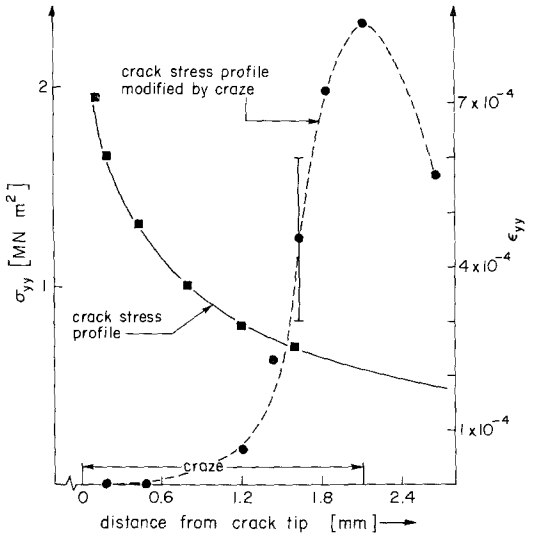

Figure 9 Stress and strain profile versus distance from crack tip along a line parallel to a propagating *n*-heptane craze.

vicinity of the craze tip is undoubtedly higher. The corresponding strain and stress profiles for the case of a *n*-heptane craze propagating out of a starter crack are shown in Fig. 9. Again the strains and stresses are calculated at a line $y = 0.32$ mm from the craze. A typical errorbar for the strain measurements is indicated. A large decrease in stress is apparent behind the craze tip. Almost no stress is borne by the craze and no strain hardening can be observed along the craze. In front of the craze tip the stress increases strongly and produces a stress concentration of approximately 4.0, which is considerably larger than that of the methanol craze.

4.2. Holographic interferometry of static crazes

4.2.1. Definitions and experimental procedures

To shed more light on the differing mechanical behaviour of solvent crazes in PS, the mechanical response of dry, static crazes is investigated. Crazes are grown under *n*-heptane or methanol in the same type of specimen as before. Then the crazes are thoroughly dried under strain. In the case of the methanol craze the notch is machined off. For *n*-heptane crazes the notch is not machined off, but kept as small as possible, because the machining may cause breaking of the craze. The specimen is inserted in the strain frame and a tensile prestrain is applied. Between exposures of the DEH, a small increment of the tensile strain is made.

The techniques used to evaluate the resulting fringe pattern have been demonstrated previously for the case of dry ethanol crazes in PC [2]. Since the opening of a crack under an incremental strain is independent of the prestrain, we have used the opening of a crack of the same length as our dry solvent crazes to normalize the craze opening displacement. The fact that cracks open linearly with the applied load makes it possible to compare the craze opening with a crack opening at a different incremental strain by just scaling the measured crack opening to the incremental strain at which the craze opening is measured. For details see [2].

4.2.2. Craze opening displacement of static crazes

The results of the incremental strain measurements show another profound difference between the mechanical properties of *n*-heptane and methanol crazes. The normalized craze opening u_{craze}/u_{crack} under incremental strain is plotted in Fig. 10 versus the normalized distance z/a from the craze tip where a is the craze length. The fringe patterns at typical prestrains are shown as inserts for each curve. Curves (a) and (b) give the normalized openings of a methanol craze, where (a) is typical of both low and high prestrains and (b) corresponds to a medium prestrain. The methanol craze opening at all prestrains is substantially smaller than the crack opening. In addition the craze opening does not depend linearly on the prestrain. At low and high prestrains the craze hardly opens up at all and the only significant opening is at its base. However, this opening is only a quarter of the opening of the methanol craze at its base at intermediate prestrains. The large opening of the craze near its base may be due to a 'thinning-out' of the fibril structure in the region of high stress at the tip of the precrack from which the craze was grown.

These results suggest that the fibrils of the dry methanol craze undergo a yielding and strain-hardening process when deformed, as proposed for ethanol crazes in PC by Peterson *et al.* [2]. The base of the craze opens gradually until a prestrain is reached where yielding of the fibrils at the base starts, thus distributing the stress more to fibrils towards the tip. Subsequently, these fibrils will also yield causing large craze openings at intermediate prestrains. The highly stretched fibrils that have yielded undergo strain-hardening which hinders further opening of the craze at high prestrains. These observations imply that the methanol

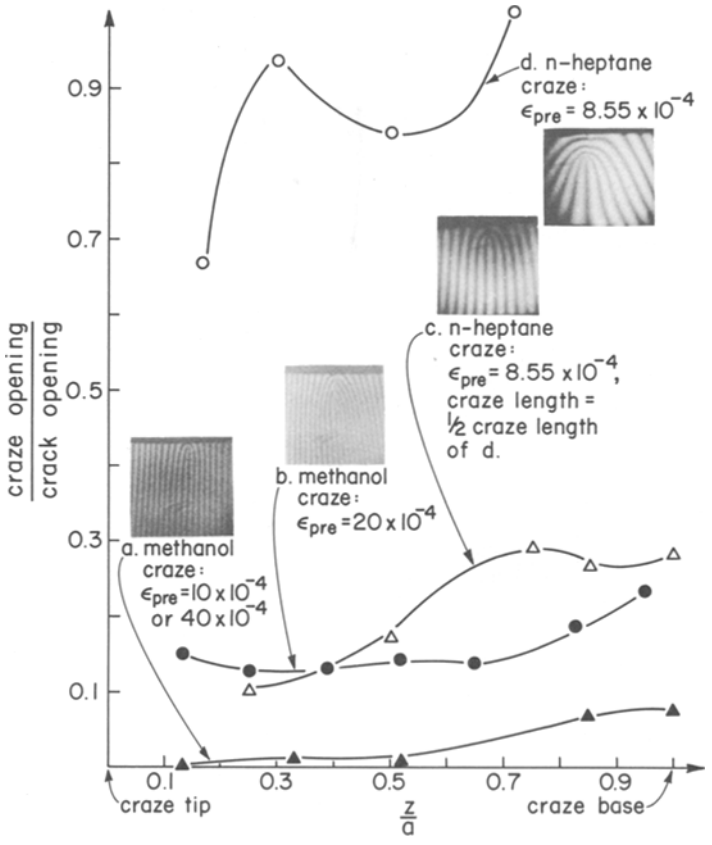

Figure 10 Normalized craze opening displacement of static *n*-heptane and methanol crazes versus normalized craze length.

craze in PS has a stress–strain curve similar to that found by Kambour and Kopp for ethanol crazes in polycarbonate [9], and by Hoare and Hull for air crazes in PS [10]. A large tangent modulus at low strains is followed by a flat plateau where small stress increases cause large strain increases. The plateau is followed by another region of high tangential modulus due to the strain hardening of the fibrils.

Dry *n*-heptane crazes behave quite differently. Fig. 10, curves (c) and (d) show the normalized craze opening for two *n*-heptane crazes. The craze length of (c) is half the craze length of (d). In both cases the incremental craze opening is independent of the prestrain. Short *n*-heptane crazes show smaller opening displacements than longer *n*-heptane crazes. Curve (c) shows that the opening of the short *n*-heptane craze is approximately equal to that of the methanol craze at intermediate prestrains. The long *n*-heptane craze opens almost as much as a crack, the tip sections showing somewhat less normalized opening than the base. Nevertheless, these long crazes are definitely true crazes, because craze fracture can be detected at higher prestrains by an audible "ping" noise which accompanies it.

4.3. Fracture mechanics of static crazes

Fracture mechanics testing of crazed specimens has been used to obtain a quantitative measurement for the strength of dry *n*-heptane and methanol crazes in PS. Methanol crazes are grown from precracks following the procedure described above and are dried for 12 h under load. The uncrazed edge of the specimen is machined away so that the specimen is cracked and crazed through its entire cross-section. The gauge length of these rectangular strip specimens is 170 mm. They are pulled in an Instron tensile machine at a nominal strain-rate of $5 \times 10^{-5}\,\text{sec}^{-1}$. The stress intensity factor for failure of methanol crazes is $K_{IC} = 1.2 \pm 0.3\,\text{MN m}^{-3/2}$. For comparison, precracked but

uncrazed specimens are tested at the same strain-rate. These specimens break at $K_{IC} = 2.69 \pm 0.05\,MN\,m^{-3/2}$.

n-heptane crazes are prepared by propagating a single craze directly out of the starter notch and are dried in the strain frame. They are tested in place, not in the Instron machine, because handling of the crazed specimen can result in premature breaking of the craze. The specimens have craze length to specimen width ratios from 0.05 to 0.5. The specimens are strained by slowly turning the micrometer until audible craze fracture occurs. The critical stress intensity factor is determined from the notch length and the fracture load which is calculated at craze fracture from the micrometer displacement. Unlike the methanol crazes the *n*-heptane crazes show K_{IC}s which decrease with increasing craze length as shown in Fig. 11. The shortest and strongest *n*-heptane craze breaks at $K_{IC} = 0.18\,MN\,m^{-3/2}$ which is only ~7% of that of the uncrazed specimen. This weakness of the *n*-heptane crazes is consistent with their crack-like SERR and their large craze opening under incremental strain.

5. Discussion

Various models of the micromechanical response of the propagating craze have been previously proposed. Narisawa and Kondo [11] have claimed, for example, that there is no stress concentration at the tip of a growing craze, a claim that is clearly contradicted by the present results on both methanol and *n*-heptane crazes. Knight [12], on the other hand, has assumed that the opening displacements of the propagating craze are constant at distances greater than a certain distance from the craze tip an assumption which is not borne out by our measurements on either type of craze. Bevan and Andrews [1] have proposed an equivalent crack model, in which the craze is represented by a crack of shorter length that is independent of applied stress. While this model may appear appropriate for the methanol crazes grown at high K_Is since the craze opening displacements in Fig. 7 are almost those of a crack near the craze tip, crazes grown at lower K_Is do not show such large tip openings. Furthermore since the range of K_Is in Fig. 6 are generated by varying the applied stress and holding the precrack length approximately fixed, the Bevan/Andrews version of the equivalent crack model would predict a single equivalent crack length for the crazes represented in Fig. 6 and thus a strain energy release rate that is a constant fraction of the strain energy release rate of the precrack at all K_Is. The pronounced minimum in the plot of $G_{craze}/\langle G\rangle_{crack}$ versus K_I^2 contradicts this prediction. It is likely this minimum arises from changes in the load-bearing capacity of fibrils within the craze with the stress intensity factor of the precrack but a detailed examination of this problem awaits the determination of the craze strain profile, which requires simultaneous craze thickness and craze opening displacement measurements.

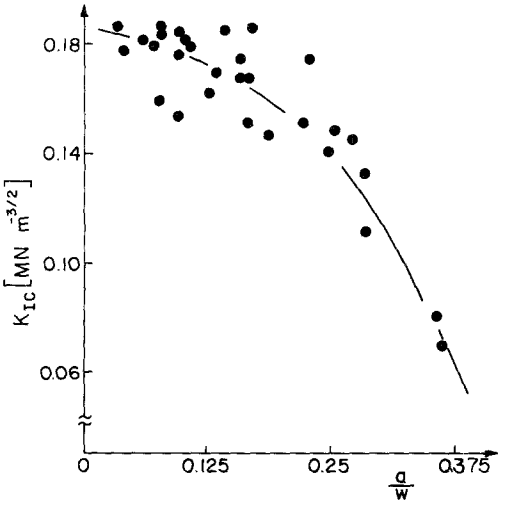

Figure 11 Critical stress intensity factor K_{IC} of *n*-heptane crazes versus craze length to specimen width ratio *a/w*.

In any event one cannot conclude that from the fact that the equivalent crack model is inappropriate for methanol crazes in PS that the model is inappropriate for other crazes including the ethanol/PMMA crazes studied in detail by Bevan and Andrews. If we have shown anything in this paper it is that crazes grown with different conditions can have profoundly different mechanical properties. These mechanical differences must be due to differences in the structure and properties of the fibrils in the craze. In the following paper we show that these structures of *n*-heptane and methanol crazes in PS are very different and we propose a simple model to account for these differences.

This work shows that DEH is a convenient tool to investigate craze deformation parameters. The stress profile of a propagating craze, for example, can not be determined easily by any other method when small stress changes are involved. Attempts are now being made to increase the fringe resolution

close to the craze therefore increasing the accuracy of measurement of the stress profile and the craze opening of the propagating craze.

Acknowledgements

The financial support of the National Science Foundation through the Cornell Materials Science Center and the US Army Research Office-Durham is gratefully acknowledged. We also thank J.A. Deroner for experimental help in measuring the strength of static crazes.

References

1. E. H. ANDREWS and L. BEVAN, *Polymer* **13** (1972) 337.
2. T. L. PETERSON, D. G. AST and E. J. KRAMER, *J. Appl. Phys.* **45** (1974) 4220.
3. G. R. IRWIN, "Fracture, Handbuch der Physik", Vol. VI (Springer, Berlin, 1958).
4. W. R. BROWN, JUN. and J. E. SRAWLEY, ASTM STP No. 410, Am. Soc. Test. Mater. (1969).
5. Earthquake Engineering Research Center, Report No. EERC 73-11, June 1973.
6. A. S. KOBAYASHI, "Experimental Techniques in Fracture Mechanics" (SESA, Westport, Conn., 1973).
7. H. R. BROWN and I. M. WARD, *Polymer* **14** (1973) 469.
8. R. BUBECK, Ph.D. Thesis, Cornell University (1976).
9. R. P. KAMBOUR and R. W. KOPP, *J. Polymer Sci.* 7 (1969) 183.
10. J. HOARE and D. HULL, *Phil. Mag.* **26** (1972) 443.
11. I. NARISAWA and T. KONDO, *J. Polymer Sci.* **11** (1973) 223.
12. A. C. KNIGHT, *ibid* **A3** (1965) 1845.

Received 30 March and accepted 3 May 1976.